I-LOAM: Intensity Enhanced LiDAR Odometry and Mapping

Yeong Sang Park[1], Hyesu Jang[1] and Ayoung Kim[1*]

Abstract— In this paper, we introduce an extension to the existing LiDAR Odometry and Mapping (LOAM) [1] by additionally considering LiDAR intensity. In an urban environment, planar structures from buildings and roads often introduce ambiguity in a certain direction. Incorporation of the intensity value to the cost function prevents divergence occurence from this structural ambiguity, thereby yielding better odometry and mapping in terms of accuracy. Specifically, we have updated the edge and plane point correspondence search to include intensity. This simple but effective strategy shows meaningful improvement over the existing LOAM. The proposed method is validated using the KITTI dataset.

I. Introduction

Together with cameras, light detection and ranging (LiDAR) has been highlighted for many years by capturing structural information around a mobile platform. Despite the high cost, LiDAR produces accurate and direct measurements around the environment providing a 2D or a 3D point cloud. This accurate range measurement and invariance to the perceptual aliasing enabled the LiDAR to be widely when detecting surrounding objects for autonomous cars, analyzing the urban environment [2], and enhancing images [3].

The relative motion inference from LiDAR-to-LiDAR matching is initially found in Iterated Closest Point (ICP) method and its variance. In this classical scan matching approach, the authors solve for the relative motion between two sets of a point cloud. For example, [4, 5] introduced efficient LiDAR matching. Recently, [6] proposed a phenomenal solution to estimate ego-motion from a sequence of LiDAR measurements. In this work, they relied on edges and planes from LiDAR points to avoid misbehavior induced from the ambiguity. In doing so, superior accuracy can be achieved in comparison to image-based visual odometry. A combination of LiDAR with other sensors mainly focused on using a camera together with LiDAR. Later, Zhang et al. [7] presented Depth Enhanced Monocular Odometry (DEMO) by exploiting depth measurement from LiDAR in the camera motion estimation.

LiDAR intensity has also been widely studied in the other literatures. Several studies examined LiDAR intensity calibration and its application to road information detection [8, 9, 10]. Others started to more actively leverage intensity in their algorithm [11]. For example, [11] additionally considered LiDAR intensity to the existing SHOT descriptor [12]. In their work in [11], authors presented intensity utilization that improves the existing LiDAR descriptor.

In this work, we introduce, I-LOAM, incorporating intensity value from LiDAR to existing LOAM algorithm and thereby improve the performance. The proposed method presents (1) modified edge and plane cost that robustness and accuracy are improved with intensity and (2) outperformance over KITTI dataset against the existing LOAM algorithm.

II. Method

We present I-LOAM to use the intensity information of LiDAR for registration. Unfortunately, the intensity may vary over time depending on the projection angle of the LiDAR ray, the material of the reflected object, and the particles in the air. This means that the intensity information has less consistency than range measurements. However, if the sensor is moved for a short period of time, we can assume the overall consistency of intensity which then can be used to obtain better results than using LiDAR geometric information only. In this paper, we propose a method of using intensity information in odometry and mapping module of Advanced LiDAR Odometry and Mapping (A-LOAM). Overall process of the proposed method is depicted in Fig. 1

A. LiDAR odometry with intensity

LOAM solves for ego-motion and mapping, given a sequence of point cloud $\mathcal{P}_k$. In the ego-motion estimation, LOAM defines the edge and plane features from the point cloud and applies cost function depending on the feature types. Following the same notation in [1], the authors computed $d_{\mathcal{E}}$ for edge points and $d_{\mathcal{H}}$ for plane points.

For this cost computation, they first need to compute the correspondences. In [1], the authors relied on the geometric distance. The points closest to the features in the current sweep's pointcloud $\mathcal{P}_k$ were found in $\mathcal{P}_{k+1}$ and matching was performed. Differing from them, we modified this correspondence search scheme to include intensity consistency. The cost was created through (1) to consider whether the intensity, as well as the distance, were similar, and then the point with the higher cost was set to have high correspondence.

$$
\begin{aligned}
d_i &= \sqrt{(\mathbf{x}_i - \mathbf{x}^L)^T(\mathbf{x}_i - \mathbf{x}^L)} \\
d_i^I &= \left\| I_i - \bar{I} \right\| \\
w_i^o &= e^{-(d_i + d_i^I)}
\end{aligned}
\tag{1}
$$

Here, $\mathbf{x}$ is 3D coordinates of a surrounding point, $\mathbf{x}^L$ is the corresponding 3D coordinates of an edge feature or a surface feature, $\bar{I}$ is intensity of the the corresponding point.

[1]Y. Park, H. Jang and A. Kim are with the Department of Civil and Environmental Engineering, KAIST, Daejeon, S. Korea [pys0728k, iriter, ayoungk]@kaist.ac.kr
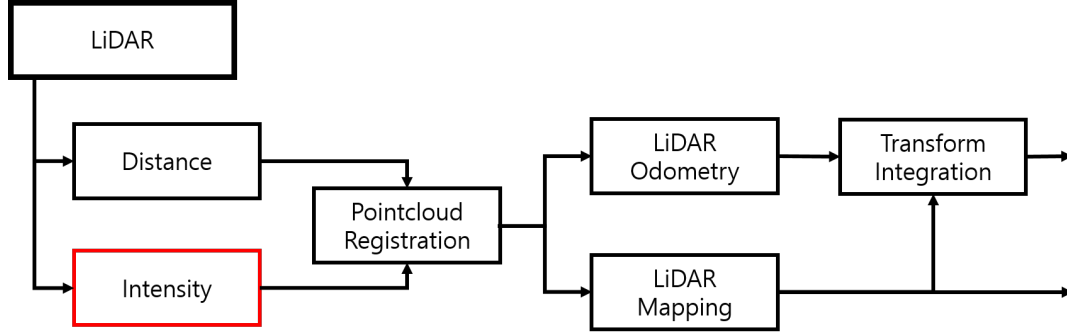
Fig. 1: Diagram of the proposed method. The existing method only utilized range data of LiDAR, however, we included intensity information in the registration step. Both distance and intensity value from LiDAR complementarily affect calculating corresponding points.

B. LiDAR mapping with intensity

Next, in the LiDAR mapping module, LOAM calculates eigenvalues $\mathbf{V}$ and eigenvectors $\mathbf{E}$ after calculating covariance of N points around feature points to register the accumulated features used in LiDAR odometry. In the edge feature, one eigenvalue is much larger than the other two eigenvalues, and the eigenvector corresponding to the largest eigenvalue represents the orientation of the edge. In the planar feature, one eigenvalue is much smaller than the other two eigenvalues, and the eigenvector corresponding to the smallest eigenvalue represents the planar orientation.

We also focused on that this covariance with the surrounding points of the feature point can be seen as important information for classifying the feature. Therefore, we propose the intensity-incorporated covariance calculation. Originally, (2) is a formula for calculating the covariance $\mathbf{M}$ of the pointcloud on three-dimensional coordinates in general.

$$\mathbf{M} = \sum_{i=1}^{N} (\mathbf{x}_i - \overline{\mathbf{x}})(\mathbf{x}_i - \overline{\mathbf{x}})^T \tag{2}$$

, where $\mathbf{x}$ is 3D coordinates of a surrounding point, $\overline{\mathbf{x}}$ is center point of the surrounding points.

In this paper, points that have similar intensity to the feature point among the nearest N points are considered to impose higher weight. Which means that points have higher probability of being associated with the feature point. Otherwise, points with large differences in intensity are distinguished by low correspondence and are given low weight. We use weighted covariance to reflect these correspondences in the optimization. As a result, (3) shows the equation of the weighted covariance matrix $\mathbf{M}^*$.

$$w_i^m = \exp\left(-\left\|I_i - \overline{I}\right\|\right)$$
$$\mathbf{M}^* = \frac{1}{\sum_{i=1}^{N} w_i^m} \sum_{k=1}^{N} w_i^m (\mathbf{x}_i - \overline{\mathbf{x}})(\mathbf{x}_i - \overline{\mathbf{x}})^T \tag{3}$$

In LOAM, the unit norms of the plane were calculated using the points around the planar feature. The dot product of the unit norm and feature point means the distance between plane and feature which is to be minimized. When the unit norm of the plane is calculated, the existing least square problem is converted into the weighted least square problem form, such as (4). The equation gives higher weight to the surrounding point which has lower intensity difference with the feature point.

$$\operatorname*{argmin}_{\beta} \sum_{i=1}^{m} w_i^m \left| y_i - \sum_{j=1}^{n} \mathbf{x}_{ij}\beta_j \right|^2 \tag{4}$$

, where y is distance between feature points and corresponding points and β is transform of feature points in accumulated scan.

As introduced the correspondence search proposed in this paper is simple but effectively encapsulates the additional intensity information during matching.

III. RESULTS

The proposed algorithm was evaluated using a KITTI odometry benchmark. Evaluations were tested running on a desktop PC with an Intel i7-7700K CPU and 32GB of RAM. Fig. 2 shows the qualitative result of applying the proposed method to sequence 00, 05, and 09 of the KITTI dataset. The quantitative result in all sequences is given in Table I. For each sequence, we examined the three cases, (*i*) A-LOAM, (*ii*) I-LOAM with only weighted covariance to edge features in mapping, and (*iii*) I-LOAM with all modules.

The proposed method using entire modules showed better results than the other methods. The difference may seem subtle in Fig. 2 while Table I shows the improvement made by the proposed method over existing A-LOAM. Intensity-incorporated module configured improved performance although the sensor has smaller field of view (FOV), or the geometric information is insufficient.

The Velodyne HDL-64E LiDAR used in the KITTI odometry dataset has $360°$ horizontal and $26.8°$ vertical FOV. Vertical FOV is about 13.4 times smaller than horizontal FOV, and it can be predicted that the vertical accuracy will be improved. As a result, in the trajectory graph, the accuracy of the x-axis and z-axis is lower than that of A-LOAM, whereas the accuracy of the y-axis (downward

TABLE I: Quantitative results for all KITTI odometry sequences. Bold letter means best performance in specific sequence. WLS stands for weighted least square.

| Seq. num.	Translation (%)			Rotation (deg/m)		
	A-LOAM	I-LOAM (weighted. cov.)	I-LOAM (weighted cov.+ wls)	A-LOAM	I-LOAM (weighted cov.)	I-LOAM (weighted cov. + wls)
0	0.9707	0.8491	**0.7067**	0.00735	0.00724	**0.00655**
1	2.7507	2.7556	**2.5019**	0.00959	0.00970	**0.00853**
2	**4.9056**	4.9071	5.0446	0.02704	**0.02690**	0.02720
3	**1.2190**	1.2258	1.2345	0.01058	0.01068	**0.01038**
4	1.3521	1.3262	**0.9090**	0.00670	0.00680	**0.00323**
5	0.6289	0.6228	**0.5116**	0.00508	0.00496	**0.00480**
6	0.6106	0.6041	**0.6012**	0.00589	0.00588	**0.00585**
7	0.4825	**0.4588**	0.4896	0.00660	**0.00613**	0.00775
8	1.1715	1.1780	**1.1261**	0.00756	0.00748	**0.00656**
9	1.1088	1.1062	**0.9106**	0.00750	0.00774	**0.00551**
10	1.5781	1.5531	**1.3133**	0.00818	0.00808	**0.00641**
Avg.	1.9897	1.9598	**1.9091**	0.01183	0.01174	**0.01126**
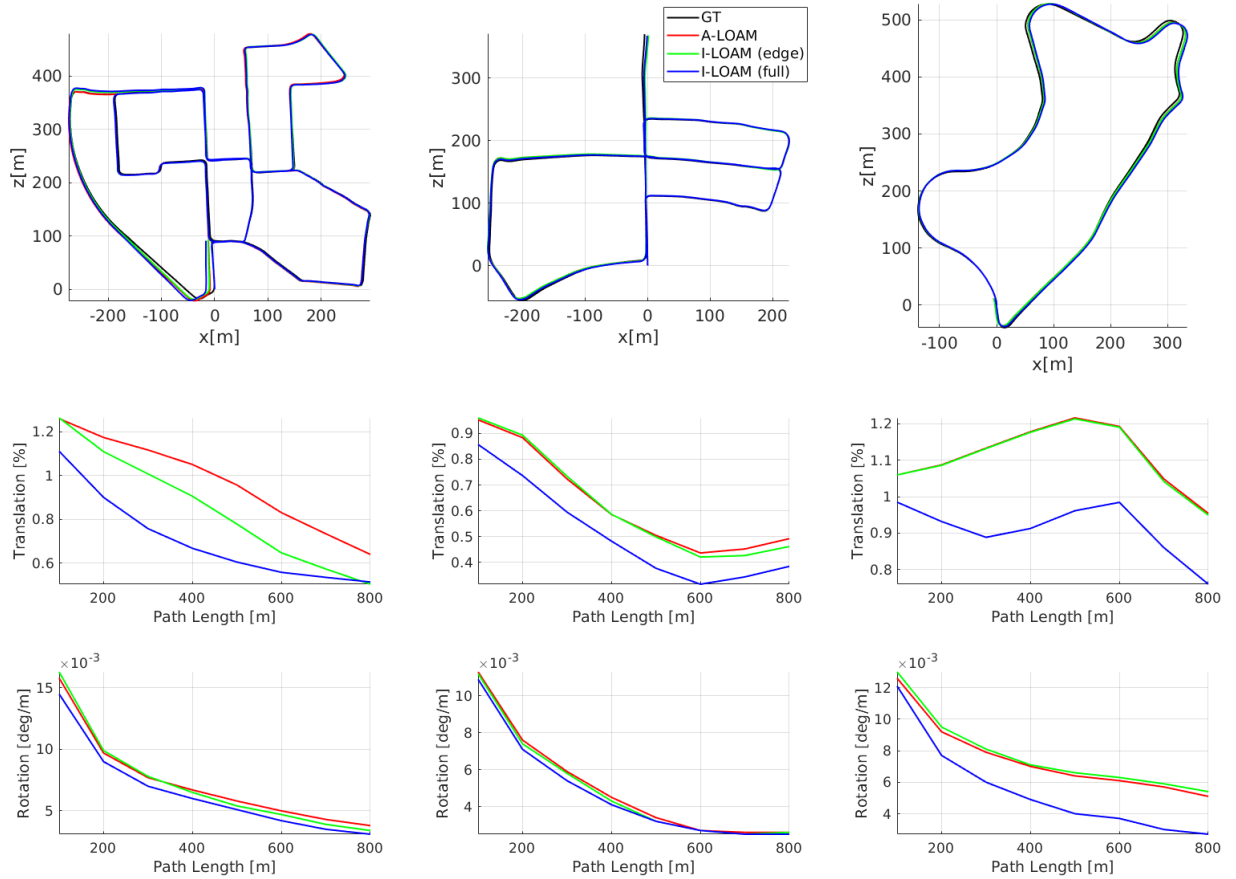
Fig. 2: Results for 00, 05, and 09 KITTI odometry sequences. A-LOAM, I-LOAM using only weighted covariance to edge feature, and I-LOAM using full module are compared against ground truth (GT). Each row shows trajectory, translation error, and rotation error graph, respectively.

being the positive direction) is greatly improved, reducing the overall translation error. Despite the KITTI dataset is mainly composed of planar moving, this y-directional component is associated with the elevation difference of the ground and thus critical to inference errors.

Table I is the result from the entire KITTI odometry dataset sequences. The performance of the proposed method outperformed A-LOAM in most sequences except sequence 02 and 03. The proposed method was on a par with A-LOAM in Sequence 03. Sequence 02 includes straight roads

and causes A-LOAM to fail in estimation translation. When this initial odometry and mapping fail in A-LOAM, the appended intensity-based weight may worsen the overall estimation.

The computational cost of odometry was increased about 2 times from 56.4 ms in A-LOAM to 107.6 ms in I-LOAM. The computational cost of mapping was increased slightly from 103.2 ms in A-LOAM to 103.5 ms in I-LOAM. Despite this increase, the overall performance still maintained near real-time performance.

IV. Conclusion

In this paper, we introduced intensity-informed LOAM and increased odometry accuracy by proposing correspondences with intensity considered. We have modified the existing LOAM to additionally consider intensity consistency for odometry inference. For mapping, the covariance computation has weighted by the intensity value so as to imply a smaller distance when intensities are similar. Overall, the improvement was validated using publically available KITTI dataset.

References

[1] J. Zhang and S. Singh, "Loam: Lidar odometry and mapping in real-time," in *Proceedings of Robotics: Science and Systems Conference*, July 2014.

[2] G. Kim, A. Kim, and Y. Kim, "A new 3D space syntax metric based on 3D isovist capture in urban space using remote sensing technology," *Computers, Environment and Urban Systems*, vol. 74, pp. 74–87, 2019.

[3] Y.-S. Shin, Y. S. Park, and A. Kim, "DVL-SLAM: Sparse depth enhanced direct Visual-LiDAR SLAM," *Autonomous Robots*, 2019, accepted. To appear.

[4] A. Segal, D. Haehnel, and S. Thrun, "Generalized-ICP," in *Proceedings of Robotics: Science and Systems*, Seattle, USA, June 2009.

[5] J. Serafin and G. Grisetti, "NICP: Dense normal based point cloud registration," in *IEEE/RSJ International Conference on Intelligent Robots and Systems (IROS)*, Sept 2015, pp. 742–749.

[6] J. Zhang and S. Singh, "Low-drift and real-time lidar odometry and mapping," *Autonomous Robots*, vol. 41, no. 2, pp. 401–416, 2017.

[7] J. Zhang, M. Kaess, and S. Singh, "A real-time method for depth enhanced visual odometry," *Autonomous Robots*, vol. 41, no. 1, pp. 31–43, 2017.

[8] J. Jeong and A. Kim, "Lidar intensity calibration for road marking extraction," in *Proceedings of the IEEE International Conference on Ubiquitous Robots (UR)*, Honolulu, Jun. 2018, pp. 455–460.

[9] A. Hata and D. Wolf, "Road marking detection using lidar reflective intensity data and its application to vehicle localization," in *Proc. IEEE Intell. Transport. Sys. Conf.* IEEE, 2014, pp. 584–589.

[10] J. Levinson and S. Thrun, "Unsupervised calibration for multi-beam lasers," in *Experimental Robotics*. Springer, 2014, pp. 179–193.

[11] J. Guo, P. V. K. Borges, C. Park, and A. Gawel, "Local descriptor for robust place recognition using lidar intensity," *IEEE Robot. and Automat. Lett.*, vol. 4, no. 2, pp. 1470–1477, 2019.

[12] F. Tombari, S. Salti, and L. Di Stefano, "Unique signatures of histograms for local surface description," in *Computer Vision – ECCV 2010*, K. Daniilidis, P. Maragos, and N. Paragios, Eds., 2010, pp. 356–369.